Heat Transfer by Combined Conduction and Radiation in Axisymmetric Enclosures

Adnan Yücel* and Mark L. Williams†
Louisiana State University, Baton Rouge, Louisiana

Combined conductive and radiative heat transfer through a gray, absorbing, emitting, and scattering medium with internal heat generation in a finite cylindrical enclosure is analyzed. The radiative transport equation is solved by the discrete ordinates method using the DOT-IV transport code, which is coupled to a compatible control-volume-based finite-difference code for the temperature field calculations. The coupled radiative transfer and the energy equations are solved by an iterative procedure. The effects of the conduction-radiation parameter, scattering, optical thickness, and wall emissivity on the medium temperatures and surface heat fluxes are discussed.

Nomenclature

a = aspect (half-height-to-radius) ratio, H/R
I = dimensionless radiation intensity, $i/4\bar{\sigma}T_w^4$
k = thermal conductivity
N = conduction-radiation parameter, $k\beta/4\bar{\sigma}T_w^3$
Q_R = dimensionless radiative heat flux, $q_R/\bar{\sigma}T_w^4$
Q_T = dimensionless total heat flux, $q_T/\bar{\sigma}T_w^4$
r = position vector
T_w = wall temperature
U = dimensionless internal heat generation, $u\beta^{-1}/4\bar{\sigma}T_w^4$
β = extinction coefficient, $\kappa+\sigma$
ϵ = wall emissivity
θ = dimensionless temperature, T/T_w
κ = absorption coefficient
σ = scattering coefficient
$\bar{\sigma}$ = Stefan-Boltzmann constant
τ = optical distance, βs, $s=r$ or z
τ_R, τ_H = optical depths in the r-, z-direction, βR, βH
Ω = direction vector
ω = single scattering albedo, σ/β
∇_τ = dimensionless gradient operator, $\beta^{-1}\nabla$

Introduction

In the past, studies of radiative transfer have been largely restricted to one-dimensional systems. However, in many practical cases, proper modeling requires multidimensional analysis in order to obtain realistic predictions. A number of solution methods based on exact formulations (analytical, zone, Monte Carlo) or various approximations (flux, spherical harmonics, discrete ordinates) of the equation of radiative transfer have been reported in the literature.[1] One method that offers high accuracy and numerical efficiency is the discrete ordinates method.[2,3] Although it has been widely used in one-dimensional problems, the discrete ordinates method has received little attention in modeling multidimensional radiative transfer. The work of Gerstl and Zardecki[4] in the area of atmospheric radiation and that of Hyde and Truelove[5] and Fiveland[6,7] in the area of engineering heat transfer comprise the few studies undertaken in this direction.

In contrast, the discrete ordinates method has been extensively used by the nuclear community in multidimensional neutron transport analysis, which is governed by the same Boltzmann transport equation. Recently the DOT-IV discrete ordinates code, originally developed for coupled neutron-gamma transport calculations,[8] was used to study radiative transfer through gray participating media in finite axisymmetrical enclosures.[9] The discrete ordinates solutions compared well with the available exact solutions. The DOT-IV code proved to be very efficient in generating solutions using high-order quadratures. Some of the advantages offered by the DOT-IV code include 1) standard one- or two-dimensional geometries, 2) arbitrary quadrature order, 3) space-dependent quadrature and mesh, 4) nonhomogenous media, 5) anisotropic scattering, 6) multigroup capability for nongray media, and 7) modular code structure.

The analysis of radiative heat transfer is often compounded by the coupling of radiation with conduction and convection. Heat transfer by simultaneous radiation and conduction or convection is important in many engineering applications such as those involving furnaces, combustion chambers, glass manufacture, and porous and fibrous insulations. Few studies[10,11] are available in the literature on the combined conduction-radiation problem in rectangular enclosures; to the best of the authors' knowledge, a systematic study involving two-dimensional cylindrical geometry has not been reported. The present paper studies the interaction of radiation with conduction in a two-dimensional cylindrical system using the DOT-IV transport code to solve the radiation part of the problem. In doing so, the paper serves to demonstrate the compatibility of the code with the control volume formulation of the energy equation, the effectiveness of the code in predicting the divergence of the radiative flux for temperature calculations, and consequently its potential for application to convective flow problems.

Analysis

The physical system considered consists of a gray, absorbing, emitting, and scattering medium with internal heat generation inside a cylinder of radius R and height $2H$ as shown in Fig. 1. The radiative transfer equation governing the steady-state radiation intensity is given in dimensionless

Presented as Paper 86-1289 at the AIAA/ASME 4th Thermophysics and Heat Transfer Conference, Boston, MA, June 2–4, 1986; received Sept. 26, 1986; revision received Dec. 18, 1986.

*Assistant Professor, Nuclear Science Center. Member AIAA.
†Associate Professor, Nuclear Science Center.

form as

$$\Omega \cdot \nabla_\tau I(r) + I(r) = S(r) \tag{1}$$

where $I(r)$ is the intensity of radiation at a point r in the direction Ω. Under the assumption of local thermodynamic equilibrium, the radiation source term in Eq. (1) for a medium of unit refractive index is given by

$$S(r) = \{\omega \int_{4\pi} I(r,\Omega')p(\Omega\cdot\Omega')d\Omega' + (1-\omega)[\theta(r)^4]\}/4\pi \tag{2}$$

where the first term on the right-hand side is the gain of radiant energy due to radiation incident from all directions that is scattered in the direction Ω. The phase function $p(\Omega\cdot\Omega')$, which represents the probability that the incident radiation at Ω' will be scattered in the direction Ω, is assumed to depend only on the angle θ_0 between Ω and Ω'. The second term represents radiation that is emitted by the medium due to its temperature. The temperature distribution inside the medium is obtained from an energy balance on a differential volume element. The nondimensional form of the energy equation for a conducting and radiating medium with internal heat generation is

$$\nabla_\tau \cdot Q_T(r) = \nabla_\tau \cdot [-4N\nabla_\tau \theta(r) + Q_R(r)] = 4U(r) \tag{3}$$

The integration of Eq. (1) over the whole solid angle and the substitution of the resulting expression in Eq. (3) gives

$$N\nabla_\tau^2 \theta(r) + U(r) = (1-\omega)\{[\theta(r)]^4 - \int_{4\pi} I(r,\Omega)d\Omega\} \tag{4}$$

Equations (1), (2), and (4) represent the nonlinear system of integral differential equations to be solved under a given set of boundary conditions. The intensity of radiation leaving a diffusely emitting and reflecting surface is

$$I(r_w,\Omega) = \epsilon[\theta(r_w)]^4/4\pi + (1-\epsilon)[\int_{2\pi} n\cdot\Omega' I(r_w,\Omega')d\Omega']/\pi \tag{5}$$

where the first term on the right-hand side is the boundary source radiation due to surface emission and the second term represents the contribution due to reflection of incoming radiation. The wall temperature or the wall heat flux can be prescribed as boundary conditions for the energy equation.

Solution Method

The discrete ordinates method involves the discretization of the (r,Ω) phase space. To this end, a spatial mesh is introduced and a suitable set of discrete directions Ω_m with associated weights w_m, $m=1,2,\ldots,M$ is selected. In two dimensions, the relation between the total number of directions M and the order N of the method is

$$M = N(N+4)/2 \tag{6}$$

The discrete ordinates equations can be derived either directly from the continuous transport equation [Eqs. (1) and (2)] or from a basic particle (photon/neutron) balance for a finite cell centered at a point (r,Ω_m). The two-dimensional discrete ordinates transport equation in standard two-dimensional geometry can be written as

$$\mu_m(A_{i+1}I_{i+1} - A_iI_i) + \xi_m B_j(I_{j+1} - I_j) + (C_{m+1}I_{m+1} - C_mI_m) + I\,V = S\,V \tag{7}$$

where A, B, and C are cell boundary geometric parameters, V is the cell volume, I the cell average (center) intensity, and μ and ξ the respective direction cosines. The first two terms on the left side of Eq. (7) represent the loss of radiant energy from the cell volume across the spatial boundaries, while the third term is an angular redistribution term due to the curvature effect ($C=0$ for $x-y$ geometry). The last term on the left is the loss by absorption and scattering. The source term on the right side of Eq. (7) includes gains due to emission and in-scatter from all directions.

The next step in the discrete ordinates formulation is the use of interpolation relations between the cell center and the cell boundary intensities in order to reduce the number of unknowns in Eq. (7). Various interpolation schemes are available; the choice is generally dictated by the physical nature of the problem. Five interpolation models are built in the DOT-IV code. With the introduction of interpolation relations into Eq. (7), the resulting discrete ordinates equations can be solved in the direction of photon travel on the spatial mesh. A detailed description of the discrete ordinates method can be found in Ref. 3.

In the specification of boundary conditions, DOT-IV allows, among others, a diffusely reflecting surface ("albedo" reflection boundary condition) or a purely emitting surface ("fixed boundary source" condition), but not one where simultaneous reflection and emission takes place. In order for DOT-IV to treat such surfaces, the reflective and emissive contributions to the outgoing intensity [see Eq. (5)] have to be considered separately. The reflected component is directly handled by specifying an albedo boundary condition at the wall. The emitted contribution is superposed indirectly using the DOT-IV feature which allows fixed sources to be specified at internal mesh surfaces. Hence wall emission is introduced as an "interior" boundary source at a grid location adjacent (e.g., within 1/1000th of a mean free path) to the wall.

Since the DOT-IV code employs cells or control volumes for spatial discretization, it is compatible with many of the algorithms currently being used for flow and temperature calculations. A standard finite-difference code based on the control volume formulation and source term linearization is used to solve the energy equation.[12] The solution procedure is outlined below:

1) An initial temperature distribution is assumed.

2) With the given temperature field, the emission term in Eq. (2) is determined. The radiative transfer equation is solved, and the incident radiant energy term for the energy equation is generated.

3) The discretized energy equation is solved by a line-by-line iterative method to obtain a new temperature distribution.

4) A new iteration is completed by repeating steps 2 and 3. The procedure is continued until pointwise convergence on temperature, etc., is obtained.

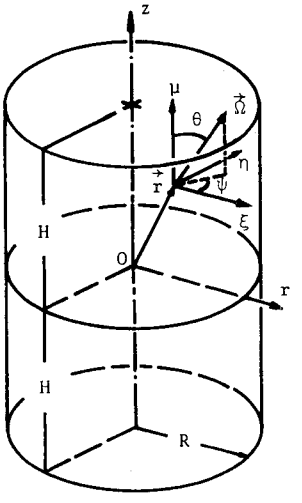

Fig. 1 Physical system under consideration.

Results and Discussion

The cases examined involve a gray, absorbing, emitting, and scattering medium with uniform heat generation. The walls of the cylindrical enclosure are assumed to be diffusely emitting and reflecting, of the same emissivity value ϵ, and maintained at a uniform temperature T_w. Hence the temperature distribution is symmetrical with respect to the midplane at $z=0$. A uniform 15×15 mesh and the fully symmetric $S4$ quadrature were found to be sufficient in all cases. A list of the quadrature directions used and the associated weights can be found in Ref. 7. Quadrature sets for several orders are available in Ref. 13. The weighted diamond difference interpolation option was used in the DOT-IV calculations. A typical problem with an optical thickness of unity required 8–12 iterations of the outlined procedure for convergence to three decimal points. Optically thicker systems require more iterations. The total CPU times ranged from 18–30 s on the LSU IBM 3084 machine. It should be noted that DOT-IV has also been optimized to execute very efficiently on vector computers. An impressive improvement in CPU time is possible if calculations are performed on a computer such as the CRAY, which takes advantage of the DOT-IV vectorization programming style.

Figure 2 shows the effect of the conduction-radiation parameter N on the midplane ($z=0$) temperature distributions for a nonscattering medium in a finite length ($\tau_R=\tau_H=1$) cylinder and in an infinitely long ($\tau_R=1$, $\tau_H\to\infty$) cylinder. The conduction-radiation parameter is representative of the relative magnitudes of the conductive and radiative modes of heat transfer. For low values of N, radiation is the dominant mode of energy transfer: the corresponding temperature profiles are very similar to that for a purely radiating medium ($N=0$), except near the wall. A temperature slip at the wall is observed in the latter case. However, there is no discontinuity in the temperature for a conducting medium. Consequently, temperatures fall sharply near the wall for small values of N. Temperature levels in a finite cylinder for a specific value of N are lower than those in the corresponding one-dimensional case. Midplane temperatures at selected radial positions are tabulated for different values of N in Table 1.

The radiative and the total (radiative plus conductive) heat fluxes along the side wall are presented in Fig. 3 for different values of N. The effect of the conduction-radiation parameter on the total heat flux is not as pronounced as that on the medium temperature. With increasing N, the total heat flux increases near the midplane and decreases near the top surface. However, the relative magnitude of the radiative flux decreases sharply as conduction dominates for large N. Table 2 lists the total radiative and conductive fluxes at the side wall heat flux and those at the top and bottom wall (combined). In all cases, about two-thirds of the total heat generated in the enclosure ($=2\pi$) is transferred out of the side surface for the given aspect ratio of 1. The radiative and conductive heat transfer rates are comparable for the case $N=0.1$.

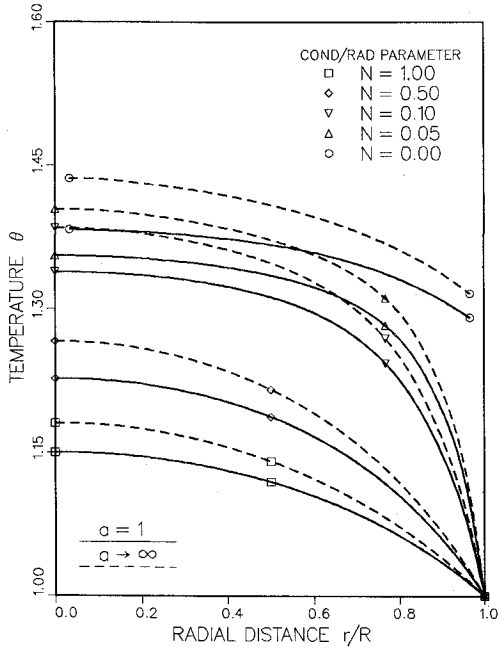

Fig. 2 Midplane ($z=0$) temperature profiles for different values of the conduction-radiation parameter ($U=1$, $\tau_R=1$, $\omega=0$, $\epsilon=1$).

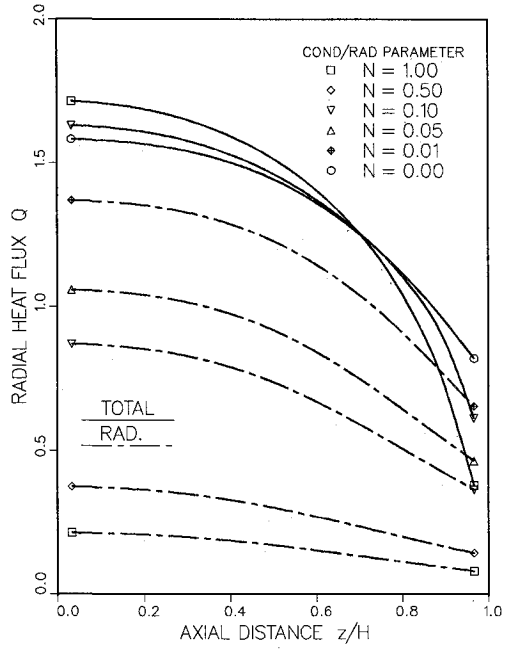

Fig. 3 Radiative and total heat fluxes along the side wall ($r=R$) for different values of the conduction-radiation parameter ($U=1$, $\tau_R=\tau_H=1$, $\omega=0$, $\epsilon=1$).

Table 1 Midplane ($z=0$) temperatures for different values of N for a cylinder with $U=1$, $\omega=0$, $\tau_R=\tau_H=1$, $\epsilon=1$

r/R	$N=1.00$	$N=0.50$	$N=0.10$	$N=0.05$	$N=0.01$	$N=0.00$
0.0	1.150	1.227	1.338	1.355	1.374	1.383
0.1	1.149	1.226	1.337	1.354	1.373	1.382
0.3	1.140	1.214	1.331	1.349	1.368	1.378
0.5	1.120	1.188	1.313	1.336	1.358	1.368
0.7	1.086	1.140	1.270	1.304	1.335	1.347
0.9	1.035	1.059	1.148	1.194	1.278	1.309
1.0	1.000	1.000	1.000	1.000	1.000	1.281

Table 2 Total radiative and conductive heat fluxes on the side wall and on the top and bottom walls (combined) for a cylinder with $U=1$, $\omega=0$, $\tau_R=\tau_H=1$, $\epsilon=1$

	Side		Top and Bottom	
N	Radiative	Conductive	Radiative	Conductive
0.00	16.96	0.00	8.17	0.00
0.01	14.35	2.61	6.89	1.28
0.05	10.72	6.24	5.13	3.04
0.10	8.63	8.34	4.12	4.04
0.50	3.56	13.48	1.68	6.41
1.00	2.01	15.06	0.95	7.11

Radial temperature profiles for different values of the scattering albedo ω are shown in Fig. 4 for an isotropically scattering medium with $N=0.1$. For a purely scattering medium ($\omega=1$), the temperature field is decoupled from the radiation field since there is no net radiative energy deposition. On the other hand, $\omega=0$ represents an absorbing and emitting medium. The interaction of radiation with conduction is greatest in this limiting case. The relative effect of scattering for $\omega<0.5$ is insignificant for the given value of the optical thickness and the conduction-radiation parameter.

Also shown in Fig. 4 are the midplane temperatures representative of a backward and a forward scattering medium for the same ω values. Overall, the effect of anisotropic scattering on the temperature distribution is found to be insignificant for a conducting and radiating medium, except for very small values of N. Similar results were observed in Ref. 14. The phase functions used for the anisotropic scattering calculations are specified in the Appendix.

The influence of the scattering albedo ω on the total heat flux is very similar to that of the conduction-radiation parameter. The total heat flux variation shown in Fig. 5 for the case $\omega=1$ represents that for a purely conducting medium with an effective heat generation rate of U/N [See Eq. (4)]. While the total heat flux remains largely unaffected, the radiative flux decreases with ω, as this implies less absorption takes place. At the same time, the conductive

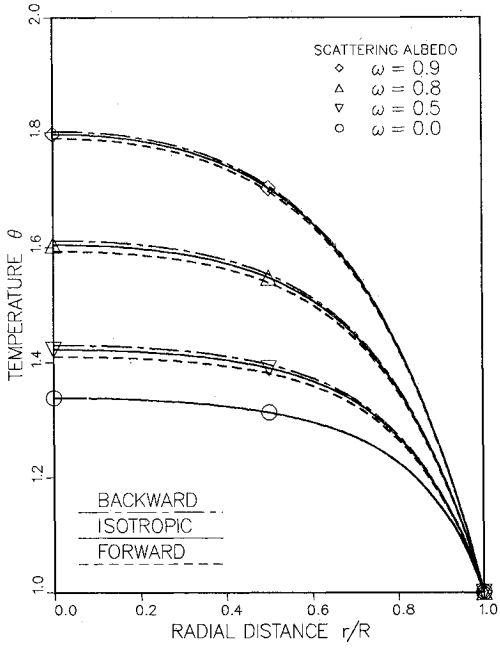

Fig. 4 Midplane ($z=0$) temperature profiles for different values of the scattering albedo ($U=1$, $N=0.1$, $\tau_R=\tau_H=1$, $\epsilon=1$).

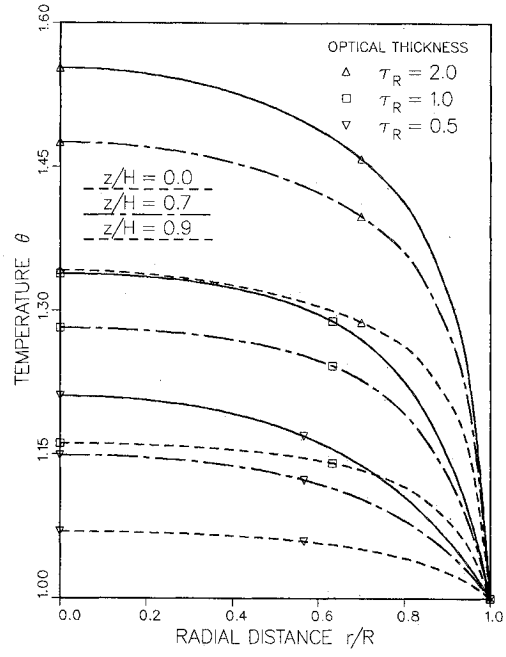

Fig. 6 Temperature profiles for different values of the optical thickness ($U=1$, $N=0.1$, $a=1$, $\omega=0$, $\epsilon=1$).

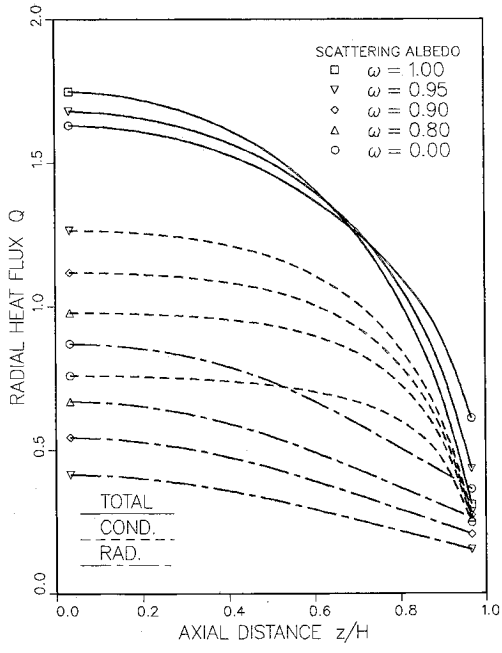

Fig. 5 Radiative, conductive, and total heat fluxes along the side wall ($r=R$) for different values of the scattering albedo ($U=1$, $N=0.1$, $\tau_R=\tau_H=1$, $\epsilon=1$).

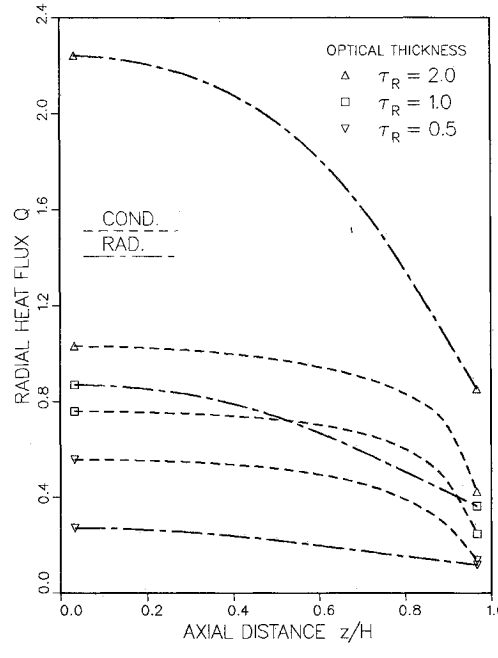

Fig. 7 Radiative and conductive heat fluxes along the side wall ($r=R$) for different values of the optical thickness ($U=1$, $N=0.1$, $a=1$, $\omega=0$, $\epsilon=1$).

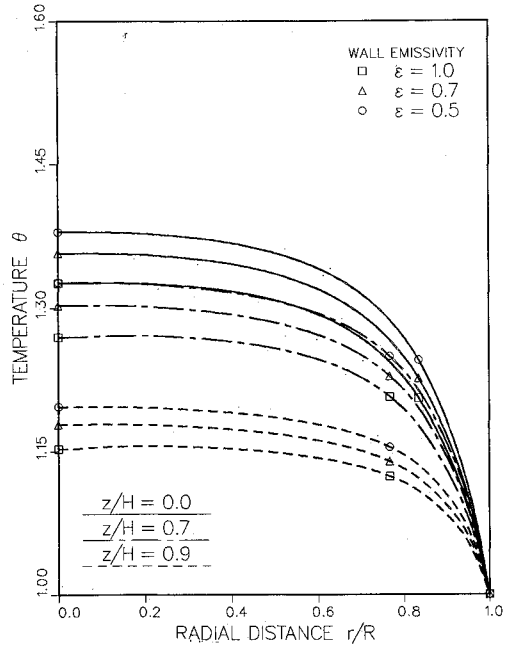

Fig. 8 Temperature profiles for different values of the wall emissivity ($U=1$, $N=0.1$, $\tau_R=\tau_H=1$, $\omega=0$).

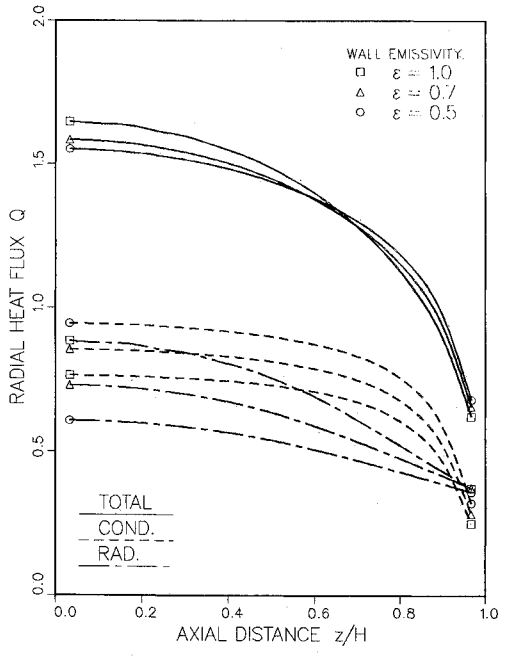

Fig. 9 Radiative, conductive, and total heat fluxes along the side wall ($r=R$) for different values of the wall emissivity ($U=1$, $N=0.1$, $\tau_R=\tau_H=1$, $\omega=0$).

contribution increases. Although not shown, the heat flux variations were also unaffected by anisotropic scattering. The effects of anisotropic scattering on the wall heat flux may be more noticeable for systems with uneven surface temperatures.[14]

The effect of the optical thickness on the temperature distribution is illustrated in Fig. 6. The optical thickness is varied by changing the enclosure dimensions in order to render U and N invariant. Thus, the total heat generated inside the enclosure increases (decreases) eightfold by doubling (halving) the optical thickness, and the medium temperatures rise (fall) accordingly. The radiative and conductive heat fluxes at the wall also show strong variations, as seen in Fig. 7. Increasing the optical path length leads to more interactions with the medium: the radiative contribution to the total wall heat flux rises from about 50% for $\tau_R=1.0$ to about 67% for $\tau_R=2.0$ but drops to 31% for $\tau_R=0.5$.

Figures 8 and 9 illustrate the effect of the wall emissivity on the medium temperatures and surface heat fluxes respectively. All surfaces are assumed to have the same emissivity value ϵ. Temperature levels are higher for enclosures with nonblack surfaces ($\epsilon<1$). Since a portion of the radiant energy incident on an emitting and reflecting boundary is reflected back into the enclosure, the net wall radiative heat flux is reduced; more heat is transferred out by conduction, which leads to higher temperature levels overall and steeper temperature gradients at the wall.

Conclusion

The DOT-IV discrete ordinates code is used to conduct a parametric study of combined radiative and conductive transfer in finite-length cylinders. DOT-IV proves to be an efficient and reliable program to predict the radiative source contribution to the energy equation. Since DOT-IV uses a control volume –based spatial discretization, it is compatible with many of the algorithms currently used to solve flow and energy balance equations. It can be readily incorporated into comprehensive codes due to its modular structure. In principle, the program can treat any complex, multiregional problem that can be modeled in standard one- or two-dimensional geometry. DOT-IV can handle nonhomogenous media with spatially varying or temperature-dependent interaction coefficients. Work is in progress to treat radiative transfer in a nongray medium using the multigroup capability of the DOT-IV code, which requires a data base of spectral interaction coefficients to be processed in multigroup form.

Acknowledgment

This work was supported, in part, by LSU Center for Energy Studies under Grant 86-01-02.

Appendix

For backward scattering, the phase function considered was

$$p(\theta_0)=8(\sin\theta_0-\theta_0\cos\theta_0)/3\pi,\ \theta_0=\cos^{-1}(\Omega\cdot\Omega') \qquad \text{(A1)}$$

which has been used to represent scattering by large particles in pulverized coal combustion.[15] In the calculations, the first three terms in the Legendre expansion of Eq. (A1) were retained. This is a very good approximation to Eq. (A1), although it attains slightly negative values for $0.9503<\mu_0<1$. The effect of this negativity, if any, is negligible as long as the scattering albedo is not very close to unity.

The Dirac-delta function approximation[16] with linear anisotropic scattering was used to represent a highly forward scattering medium

$$p(\mu_0)=2f\delta(1-\mu_0)+(1-f)\bar{p}(\mu_0),\ \bar{p}(\mu_0)=1+\bar{a}_1\mu_0,$$
$$\mu_0=\Omega\cdot\Omega' \qquad \text{(A2)}$$

with $f=0.75$ and $\bar{a}_1=0.9$. The substitution of Eq. (A2) in Eq. (2) results in a set of governing equations that are identical in form to Eqs. (1-4) but contain respectively the scaled variables $\bar{\tau}$, $\bar{\omega}$, $\bar{p}$, $\bar{U}$, and $\bar{N}$ instead of τ, ω, p, U, and N such that $\bar{\tau}=(1-\omega f)\tau$, $\bar{\omega}=(1-f)\omega/(1-\omega f)$, $\bar{U}=\bar{U}/(1-\omega f)$, and $\bar{N}=(1-\omega f)N$.

References

[1]Viskanta, R., "Radiative Heat Transfer," *Fortschritte der Verfahrenstechnik*, Vol. 22, 1984, pp. 51-81.

[2]Chandrasekhar, S., *Radiative Transfer,* Dover, New York, 1960.
[3]Duderstadt, J. and Martin, W., *Transport Theory,* Wiley, New York, 1979.
[4]Gerstl, S.A. and Zardecki, A., "Discrete-ordinates Finite-element Method for Atmospheric Radiative Transfer and Remote Sensing," *Applied Optics,* Vol. 24, 1985, pp. 81–93.
[5]Hyde, D.J. and Truelove, J.S., "The Discrete Ordinates Approximation for Multidimensional Radiant Heat Transfer in Furnaces," AERE-R 8502, 1977.
[6]Fiveland, W.A., "A Discrete Ordinates Method for Predicting Radiative Heat Transfer in Axisymmetric Enclosures," ASME 82-HT-20, 1982.
[7]Fiveland, W.A., "Discrete Ordinates Solutions of the Radiative Transport Equation for Rectangular Enclosures," *Journal of Heat Transfer,* Vol. 106, 1985, pp. 669–706.
[8]Rhoades, W.A., Simpson, D.B., Childs, R.L., and Engle, W.W., "The DOT-IV Two-Dimensional Discrete Ordinates Transport Code with Space-Dependent Mesh and Quadrature," ORNL/TM-6529, Oak Ridge National Laboratory, 1979.
[9]Yücel, A. and Williams, M.L., "Thermal Radiation Heat Transport Using Discrete Ordinates," *Proceedings, ANS Topical Conference on Theory and Practices in Radiation Protection and Shielding,* Knoxville, TN, April 22–24, 1987, Vol. 2, pp. 523–532.
[10]Ratzel, A.C. and Howell, J.R., "Two-Dimensional Radiative Transfer in Absorbing-Emitting Media Using the P-N Approximation," *ASME Journal of Heat Transfer,* Vol. 105, 1983, pp. 333–340.
[11]Razzaque, M.M., Klein, D.E., and Howell, J.R., "Finite Element Solution of Radiative Heat Transfer in a Two-Dimensional Rectangular Enclosure with Gray Participating Media," *Journal of Heat Transfer,* Vol. 105, 1983, pp. 933–936.
[12]Patankar, S.V., *Numerical Heat Transfer and Fluid Flow,* McGraw-Hill, New York, 1980.
[13]Lee, C.E., "The Discrete S_n Approximation to Transport Theory," LA-2595, 1962.
[14]Yuen, W.W. and Wong, L.W., "Heat Transfer by Conduction and Radiation in a One-Dimensional Absorbing, Emitting and Anisotropically-Scattering Medium," *Journal of Heat Transfer,* Vol. 102, 1980, pp. 303–307.
[15]Khalil, H., Shultis, J.K., and Lester, T.W., "Stationary Thermal Ignition of Particle Suspensions," *Journal of Heat Transfer,* Vol. 105, 1983, pp. 288–294.
[16]Crosbie, A.L. and Davidson, G.W., "Dirac-Delta Function Approximations to the Scattering Phase Function," *Journal of Quant. Spectrosc. Radiat. Transfer,* Vol. 33, 1985, pp. 391–409.